Biophysical Chemistry, 44 (1992) 129–137
Elsevier Science Publishers B.V., Amsterdam

BIOCHE 01683

Motions studies of the human α_1-acid glycoprotein (orosomucoid) followed by red-edge excitation spectra and polarization of 2-*p*-toluidinylnaphthalene-6-sulfonate (TNS) and of tryptophan residues

J. Albani

Laboratoire de Chimie-Biologique, Université des Sciences et Techniques de Lille, 59655 Villeneuve d'Ascq Cédex (France)

(Received 14 October 1991; accepted in revised form 7 May 1992)

Abstract

Dynamics studies on tryptophan residues of human α_1-acid glycoprotein (orosomucoid) and of 2-*p*-toluidinylnaphthalene-6-sulfonate bound to the protein are performed. Excitation at the red edge of the absorption spectrum of the tryptophan does not lead to a shift of the fluorescence emission maximum of the fluorophore. This reveals that Trp residues present motions with respect to their microenvironment. This is confirmed by polarization studies as a function of temperature. Excitation at the red edge of the absorption spectrum of TNS leads to an important shift (15 nm) of the fluorescence emission maximum of the probe. This reveals that emission of TNS occurs before relaxation of the amino-acids dipole occurs. Emission from a non-relaxed state means that TNS molecules are bound tightly to the protein, a result confirmed by polarization studies.

Keywords: Tryptophan residues dynamics; Orosomucoid–TNS interaction; Protein–fluorophore probe; Polarization studies; Dipole relaxation

1. Introduction

Dynamics of proteins are currently investigated by fluorescence anisotropy studies and by red-edge excitation shift method [1,2]. Steady state measurements of emission anisotropy are realized in function of temperature and viscosity or under conditions of oxygen quenching [3,4]. The red-edge excitation shift method allows to compare the motion of a fluorophore to that of the protein. This technique is very sensitive to changes occurring to the protein and especially in the proximity of the probe [5–7].

In this work, red-edge excitation shift and polarization experiments are applied to Trp residues of human α_1-acid glycoprotein (orosomucoid) and to the fluorophore TNS bound to the protein.

Orosomucoid is a small acute-phase glycoprotein ($M \sim 41\,000$ Da), that is negatively charged at physiological pH. It contains 40% carbohydrate in weight and has up to 16 sialic acid residues (10–14% by weight) [8]. The protein has three Trp residues, one near its surface and two imbedded in the protein matrix [8].

Excitation at the red edge of the absorption spectrum of the fluorophore molecules allows to

Correspondence to: Dr. J. Albani, Laboratoire de Chimie-Biologique, Université des Sciences et Techniques de Lille, 59655 Villeneuve d'Ascq Cédex (France).

study the flexibility of their microenvironment. We found that the emission maximum of the Trp residues does not vary with the excitation wavelength. This result reveals that the intrinsic fluorophore presents motions with respect to its microenvironment.

The emission maximum of TNS is shifted toward longer wavelengths upon changing the excitation wavelength. This means that TNS binding sites are rigid with respect to their microenvironments.

Polarization measurements as a function of temperature confirm the red-edge excitation results, i.e. Trp residues do have residual motions and TNS is bound tightly to the protein.

2. Materials and methods

Orosomucoid was extracted from human plasma and prepared as described in [9]. The lyophilized protein was dissolved in a 10 mM phosphate, 0.143 M NaCl buffer, pH 7. Its concentration was determined spectrophotometrically using an extinction coefficient of 29.7 mM^{-1} cm^{-1} at 278 nm. In all experiments, the concentration of orosomucoid was equal to 5 μM.

The concentration of TNS (from Sigma) was determined spectrophotometrically using an extinction coefficient equal to 18.9 mM^{-1} cm^{-1} at 317 nm [10].

Absorbance data were obtained with a Shimadzu MPS-2000 spectrophotometer using 1-cm path length cuvettes.

Fluorescence spectra were obtained with a Perkin-Elmer LS-5 spectrofluorometer. Bandwidths used for excitation and emission were 2.5 nm.

The quartz cuvettes used presented optical pathlengths equal to 1 and 0.4 cm for the emission and excitation wavelengths, respectively. Observed fluorescence intensities were first corrected for the dilution, then corrections were made for the adsorption with the following formula [11]:

$$F_{corr} = F_{obs}\ 10^{(OD_{ex}+OD_{em})/2}, \qquad (1)$$

where F_{obs} is the intensity corrected for the dilution, F_{corr} the intensity after correction for the absorption, and OD_{ex} and OD_{em} refer to the optical density (absorbance) at the excitation and emission wavelengths, respectively. (The OD_{ex} value was corrected to account for the 0.4 cm pathlength.) Finally fluorescence spectra were corrected for the Raman effect due to the buffer and for the fluorescence of free TNS in solution.

Polarization data were obtained with the same Perkin-Elmer fluorometer used for the emission spectra acquisition. Bandwidths used for excitation and emission were both 5 nm.

The measurement of the limiting fluorescence polarization, P_0, was done with a SPEX fluorometer at −35°C. The sample (TNS–orosomucoid or orosomucoid) was dissolved in the phosphate/NaCl buffer. A 100% ethanol solution was used as the cooling solution. The compartment holding the cuvette was flushed with cool dry air. The temperature was measured in the cuvette with a chromel–alumel probe. A value of P_0 equal to 0.24 was obtained at λ_{ex} 295 nm, a value typical of Trp residues in proteins [12], while for TNS the measured P_0 was 0.435 at λ_{ex} 320 nm.

Fluorescence lifetimes of Trp residues and of TNS–orosomucoid complex were measured by phase fluorometry using the multifrequency method. In the frequency domain, the sample under study is excited with a continuous sinusoidally amplitude-modulated light beam. In such a case, the emission intensity will be modulated sinusoidally at the excitation frequency but delayed by a phase angle (Θ) and will be amplitude-demodulated. A scatter solution is used to evaluate the phase angle delay and the amplitude demodulation.

The phase delay of the fluorescence, Φ, is then given as

$$\Phi = (\Phi_R - \Phi_F) - (\Phi_R - \Phi_S),$$

where Φ_R represents the phase of the internal electronic reference signal (reference photomultiplier) and Φ_F and Φ_S represent the measured phase readings for the fluorescent and scattered signals, respectively.

The modulation of the fluorescence M is defined as

$$M = (AC/DC)_F/(AC/DC)_S,$$

where the subscripts F and S refer to fluorescence and scattering and the AC and DC terms refer to the alternating and direct current contributions to the signal.

The lifetime measured with the phase delay is obtained from

$$\mathrm{tg}\Phi = \omega\tau_p.$$

While that obtained with the demodulation is given by

$$M = \left(1+\omega^2\tau_m^2\right)^{-1/2}.$$

A monoexponential decay gives $\tau_p = \tau_m$ and a multiexponential one gives $\tau_p < \tau_m$.

Fluorescence lifetimes from a heterogeneous emission was obtained with the multifrequency and cross-correlation method. A frequency synthesiser controls the frequency ω applied (from 1 MHz to the GHz). In the cross-correlation technique, the high frequency ω is transformed to any desired low frequency by mixing ω with a second frequency, $\omega + \Delta\omega$. The relative phase and degree of modulation of the original high frequency are uniquely preserved in the resulting difference frequency; $\Delta\omega$ is less than 100 Hz.

The mathematical treatment of the cross-correlation method is as follows:

$$F(t) = A + B\sin(\omega t - \Phi),$$

where Φ is the phase delay of the fluorescence,

$$R(t) = a + b\sin(\omega t - \varphi),$$

where φ is the phase delay of the reference signal. The resulting signal obtained at the emission photomultiplier is equal to the product $R(t)F(t)$, i.e.

$$\begin{aligned} R(t)F(t) = {} & Aa + Ab\sin(\omega t - \varphi) \\ & + aB\sin(\omega t - \Phi) \\ & + \frac{bB}{2}\cos(\Phi - \varphi) \\ & - \frac{bB}{2}\cos(2\omega t - \varphi - \Phi). \end{aligned}$$

Integration of the signal over a period of $2\pi/\omega$ gives as mean value:

$$\begin{aligned} \langle F(t)R(t)\rangle &= \omega/2\pi\int_0^{2\pi/\omega}(F(t)R(t))\,\mathrm{d}t \\ &= aA + bB\cos(\varphi - \Phi). \end{aligned}$$

φ increases linearly with the time, so that we have $\varphi = \Delta\omega t$. Thus, the mean value $\langle F(t)R(t)\rangle$ is equal to $aA + \frac{1}{2}bB\cos(\Delta\omega t - \Phi)$. At any frequency ω, the values of Φ and M are given by

$$\Phi = \tan^{-1}(S/G) \quad \text{and} \quad M = \left[S^2 + G^2\right]^{1/2},$$

where

$$G = f_i\left(1+\omega^2\tau_i^2\right)^{-1} \quad \text{and} \quad S = f_i\omega\tau_i\left(1+\omega^2\tau_i^2\right)^{-1},$$

and f_i is the fraction of the fluorescence intensity detected for the ith component and τ_i its fluorescence lifetime. For further details on the cross-correlation method see Refs. [13–15].

In this work, lifetime measurements were obtained with an automated multifrequency phase fluorometer, using the harmonic content of the pulse train of a stabilised, mode-locked, cavity dumped dye laser. Data were collected over 50 modulation frequencies. Detailed statistical techniques were introduced in the data analysis for phase fluorometry. Mean, standard deviation and percentage in the interval $[-2, 2]$ of the weighted residuals were compared with the predicted values of 0.1 and 95.5, respectively. More details are given in ref. [16].

Fluorescence intensity, $I(\lambda, t)$, of Trp residues can be adequately represented by a sum of two exponentials

$$I(\lambda, t) = 0.64\,\mathrm{e}^{-t/3} + 0.36\,\mathrm{e}^{-t/0.83},$$

where 0.64 and 0.36 are the pre-exponential factors, 3 and 0.83 the decay times and λ the emission wavelength (330 nm). The weighted average fluorescence lifetime $\bar{\tau}_0 = 2.7$ ns is used to calculate the rotational correlation time from the Perrin plot.

$$\bar{\tau}_0 = \sum f_i\tau_i \quad \text{and} \quad f_i = \alpha_i\tau_i/\sum\alpha_i\tau_i,$$

where α_i are the pre-exponential terms and τ_i the fluorescence lifetimes.

The fluorescence intensity decay of TNS bound to orosomucoid can be adequately represented by a sum of three exponentials,

$$I(\lambda, t) = 0.45\ e^{-t/11} + 0.34\ e^{-t/4.3} + 0.21\ e^{-t/0.4},$$

where 0.45, 0.34 and 0.21 are the pre-exponential factors and 11, 4.3 and 0.4 ns the decay times. The emission wavelength (λ) is 430 nm. The weighted average fluorescence lifetime $\bar{\tau}_0 = 9.33$ ns was used to calculate the rotational correlation time from the Perrin plot. The short lifetime of 0.4 ns corresponds to the free TNS [17], while long ones correspond to bound TNS. The static contributions of the components to the total fluorescence is equal to 76% and 22.5% for the bound TNS and 1.5% for free TNS in solution, respectively.

3. Theory and red-edge excitation shift

Fluorophore molecules and the amino-acids of the binding sites (case of TNS) or the amino-acids of their microenvironment (case of Trp residues) are associated by their dipoles. The dipole of the excited fluorophore has an orientation different from that of the fluorophore in the ground state. Thus dipole–dipole interaction in the ground state is different from that in the excited state. This new interaction is unstable. To reach stability, fluorophore molecules need to use some of their energy to reorient the dipole of the amino-acids of the binding site. The dipole reorientation is called the relaxation phenomenon [2]. After relaxation, fluorescence emission occurs. This is the case when relaxation is faster than fluorescence, i.e. the relaxation lifetime τ_r is shorter than the fluorescence lifetime τ_0. This happens when the binding site is flexible and the fluorophore can move easily. Displacements of TNS molecules will be representative of the time scale and amplitude of the motions of the surrounding protein matrix. Emission from a relaxed state does not change with the excitation wavelength.

When the binding site is rigid, fluorescence emission occurs before relaxation. In this case excitation at the longer wavelength edge of the absorption band photoselects population of fluorophores energetically different from the photoselected when the excitation wavelength is shorter. When the red edge excitation is performed, the energy $h\nu^{edge}$ of the electronic transition is equal to $E_e^{edge} - E_g^{edge}$, where $E_e - E_g$ refers to the difference of energy between excited and ground states; $h\nu^{edge}$ is lower than $h\nu^{sw}$, the energy of the electronic transition that occurs at short wavelengths. Thus excitation at the red edge gives a fluorescence spectrum with a maximum located at higher wavelength than that obtained when excitation is performed at short wavelengths.

Thus, the observation of red shift of $\lambda_{em,max}$, upon red shift in λ_{ex}, indicates that the system meets with the $\tau_0 < \tau_r$ condition. This means a decreased mobility of the fluorophore on its binding site with respect to the dipolar matrix of the site.

4. Results

Figure 1 shows the fluorescence spectra of TNS bound to orosomucoid obtained at four excitation wavelengths. At 360 nm, the emission maximum is located at 425 nm. It shifts to higher wavelength (430 nm and 440 nm) when excitation wavelengths are 380 and 400 nm, respectively. The red-edge excitation shift is significant (15 nm). This is taken as a direct evidence that TNS has a restricted mobility on the orosomucoid. Thus, fluorescence emission occurs before the dipole relaxation.

The dependence of the emission maximum on the excitation wavelength is plotted in Fig. 2 at three temperatures (8, 25 and 40°C). The temperature does not seem to affect the behaviour of the plot. If an increase in temperature accelerates τ_r, the magnitude of the red-edge excitation effect will be lower at high temperatures than at low temperatures, and the behaviour of the plot obtained in Fig. 2 will differ from one temperature to another.

The rotational correlation time (Φ_p) of a hydrated sphere is obtained from the equation:

$$\Phi_p = M(\nu + h)\eta / kTN, \qquad (2)$$

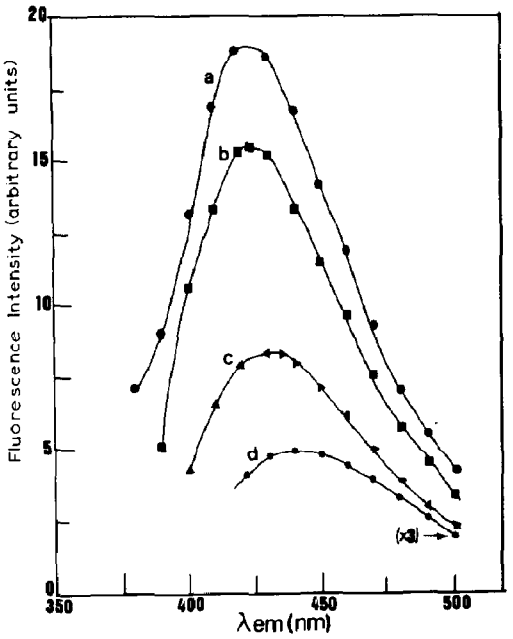

Fig. 1. Steady-state fluorescence spectra of the 2.6-TNS–orosomucoid complex recorded at four excitation wavelengths, 360 nm (a), 370 nm (b), 380 nm (c), and 400 nm (d). [Orosomucoid] = [TNS] = 5 μM, temperature = 20°C.

where M is the protein molecular weight, $\nu = 0.73$ cm^3/g the specific volume, $h = 0.3$ cm^3/g the degree of hydration and η the dynamic viscosity of the medium. At 20°C, the Φ_p value of orosomucoid is 17 ns if the protein is spherical. Neutron scattering studies indicated that orosomucoid is slightly more elongated than a globular protein, carbohydrate residues are mainly responsible for this conformation [18]. In this case, theoretical value of Φ_p is slightly higher than that calculated for a spherical protein of the same molecular weight.

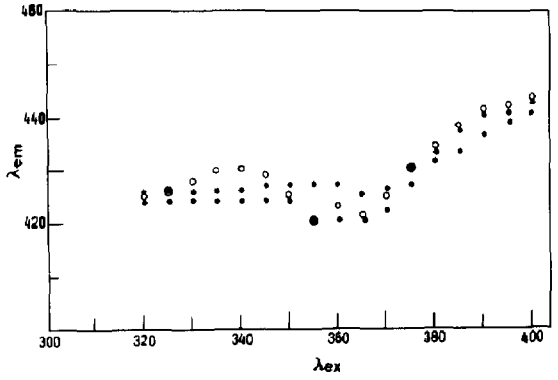

Fig. 2. Dependence of the maximum of the emission spectra on excitation wavelength of the 2,6-TNS-orosomucoid complex. [Orosomucoid] = [TNS] = 5 μM. (●) 8°C, (*) 25°C, and (○) 40°C.

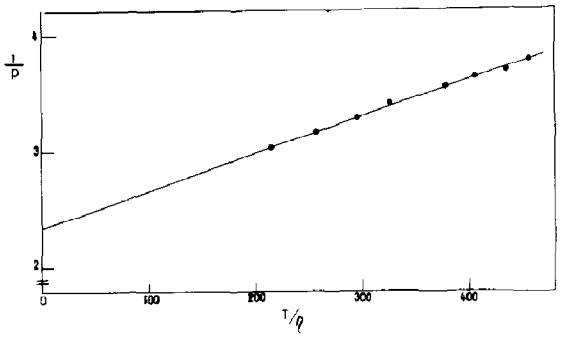

Fig. 3. Steady-state fluorescence polarization versus temperature/viscosity ratio for TNS–orosomucoid complex. Data were obtained by thermal variation of temperature. λ_{ex}, 320 nm, and λ_{em}, 430 nm.

Fluorescence polarization of TNS–orosomucoid complex ($\lambda_{em} = 430$ nm and $\lambda_{ex} = 320$ nm) is measured in function of temperature. A Perrin plot representation (Fig. 3) [19]:

$$\frac{1}{p} = \frac{1}{p_0} + \left(\frac{1}{p_0} - \frac{1}{3}\right)\frac{RT\bar{\tau}_0}{\eta V} = \frac{1}{p_0} + \left(\frac{1}{p_0} - \frac{1}{3}\right)\frac{\bar{\tau}_0}{\Phi_R} \quad (3)$$

where p and p_0 are the polarization in the presence and absence of rotational diffusion, respectively; $\bar{\tau}_0 (= 9.3$ ns), η and V are the mean fluorescence lifetime, the viscosity and the fluorophore rotational volume. From eq. (3) it is possible to obtain the rotational correlation time Φ_R of the fluorophore bound to the protein. When the fluorophore does present significant motion when bound to the protein, Φ_R will differ from the theoretical value Φ_p expected for a sphere, and the extrapolated value of p, $p(0)$, will be lower than p_0 the value measured at −35°C.

At 20°C Φ_R calculated is equal to 19 ns. This value, slightly higher than 17 ns. indicates that

TNS follows the global motion of the protein. The extrapolated p at $T/\eta = 0$ is equal 0.431 (Fig. 3). This value identical to that (0.435) found for the polarization at -35°C reveals the absence of a segmental motion.

Polarization results are in good agreement with the results obtained by red-edge excitation shift experiments, i.e. binding sites of TNS are rigid on the protein.

Figure 4 shows fluorescence spectra of Trp residues of orosomucoid obtained at three excitation wavelengths. Emission maximum located at 335 nm does not change with excitation wavelength (λ_{ex}, 295, 300 and 305 nm). This means that Trp residues microenvironments are not rigid.

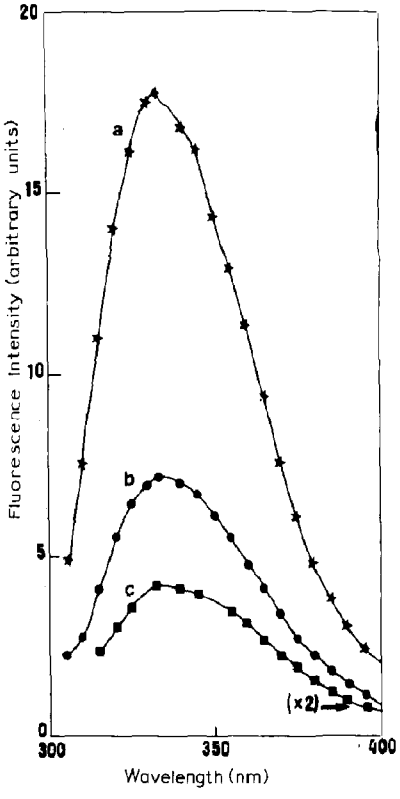

Fig. 4. Steady-state fluorescence spectra of 5 μM, α_1-acid glycoprotein (orosomucoid) obtained at three excitation wavelengths, 295 nm (a), 300 (b) and 305 nm (c). Temperature = 20°C.

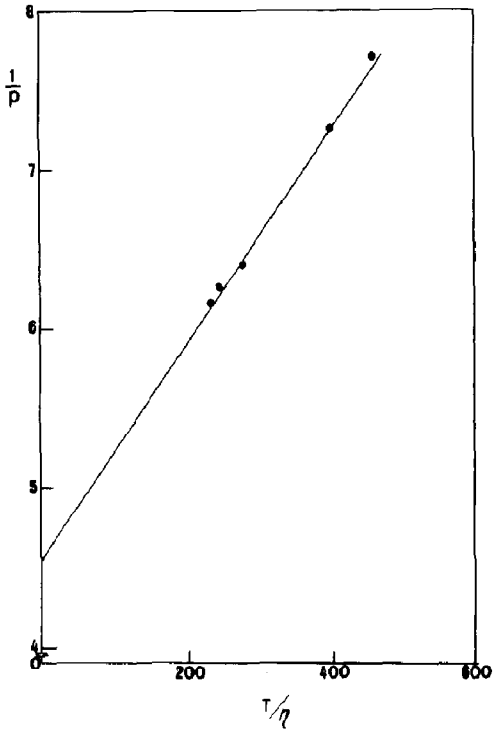

Fig. 5. Steady-state fluorescence polarization versus temperature over viscosity ratio for human α_1-acid glycoprotein. Data were obtained by thermal variations in the range 7–35°C. λ_{ex}, 295 nm; λ_{em}, 330 nm. Protein concentration is equal to 5 μM.

Steady state fluorescence polarization (λ_{em} = 330 nm and λ_{ex} = 295 nm) is performed at different temperatures. A Perrin plot representation (Fig. 5)

$$\frac{1}{p} = \frac{1}{p_0} + \left(\frac{1}{p_0} - \frac{1}{3}\right)\left(1 + \frac{\bar{\tau}_0}{\Phi_R}\right)$$

$$= \frac{1}{p_0} + \left(\frac{1}{p_0} - \frac{1}{3}\right)\left(1 + \frac{RT\bar{\tau}_0}{\eta V}\right) \qquad (4)$$

should enable us to obtain information concerning the motion of the fluorophore.

The value of $p(0)$ found from the Perrin plot is 0.219. This value, lower than that (0.24) found for the polarization p_0 at -35°C, reveals the presence of a segmental motion. This is in a good agreement with the results obtained by red-edge

excitation shift experiments, i.e. Trp residues are mobile with respect to their microenvironment.

Two motions contribute to the depolarization process, the local motion of the tryptophan residues and the global motion of the protein; the existence of local motions is revealed by an extrapolated value $p(0)$ lower than that p_0 measured in frozen solution and by an apparent rotational correlation time Φ_A lower than that expected for the global motion of the protein. Thus a fraction (α) of the total polarization is lost due to the segmental motion and the remaining polarization decays as a result of rotational diffusion of the protein.

It is possible to measure the relative importance of the mean residual motions of Trp residues,

$$p(0)/p_0 = 1 - \alpha, \tag{5}$$

where α is the residual motion of the fluorophore, and the average angular displacement Θ of the fluorophore inside the protein,

$$\cos^2\Theta = (1 - 2\alpha/3), \tag{6}$$

The values of α and Θ are 0.1 and 15°.

The rotational correlation time Φ_A (5.66 ns at 20°C), lower than that (17 ns or more) expected for orosomucoid is an apparent one and indicates that Trp residues present segmental motions independent of the global motion of the protein.

5. Discussion

Red-edge excitation shift (15 nm, Fig. 1) indicates that motions around TNS molecules are non-existent.

The behaviour of the plot ($\lambda_{em} = f(\lambda_{ex})$, see Fig. 2) is temperature independent. This result indicates that the red-edge excitation effect is not a dynamic process but a static one, i.e. TNS molecules are bound tightly to the protein. In this case, emission observed at any excitation wavelength occurs from a non-relaxed state and is temperature independent. Otherwise, raising the temperature will increase the mobility of the binding site, affecting at the same time the fluorescence of the probe.

We notice that emission maximum does not present the same position at the three temperatures. However, this change is not regular along the excitation wavelengths. For instance, at 335 nm and 340 nm, the difference of emission maxima at 8°C and 40°C is more than 30% of full range emission maxima changes, while at 320 and 395 nm, the difference is much less important. This means that the difference change observed is not the effect of optical phenomenon that interferes with fluorescence such as scatter. Otherwise, we should observe the same difference change along the plot. Also, scatter would be observed in the Perrin plots (Figs. 3 and 5) affecting the extrapolated value of p, which is not the case.

A possible explanation of the difference in the emission maximum is: the continuous irradiation of TNS–protein complex may induce a partial photodestruction of the probe site altering the position of the maximum. This photodestruction is less important at 8°C than at 25°C or 40°C. Also we used the same sample for the three temperatures, a fact that makes the TNS–protein complex more sensitive to irradiation than a sample that has been irradiated for a shorter time.

The data in Fig. 2 are affected by different experimental errors such as irradiation of the same sample for a long period of time. Reading off the intensities from the fluorescence spectra to determine the maximum can also be a source of error, especially at 35°C because of the broadness of the peaks. We may have three to five subsequent emission wavelengths around the real maximum at the same fluorescence intensity.

However, since the behaviour of the plot $\lambda_{em} = f(\lambda_{ex})$ is identical at all three experimental temperatures, it is that the red-edge excitation effect is a static process.

The rotational correlation time (19 ns) found for orosomucoid from the Perrin plot (Fig. 3) and the extrapolated polarization (0.431) confirm the red-edge excitation shift experiment, ie. the TNS binding site is rigid on the protein. The rotational correlation time (19 ns) obtained from the Perrin plot is not significantly higher than that (17 ns) expected for a globular protein of molecular weight equal to 41 000. Thus our results do not

allow to consider orosomucoid as a non-globular protein.

Absence of a red-edge excitation shift for Trp residues (Fig. 4) meets with the fact that emission occurs from a relaxed state, i.e. motions around Trp residues do exist. Furthermore, residual motion of Trp is existent as it is revealed by the different values of the extrapolated polarization at $T/\eta = 0$ and the polarization measured at -35°C.

The apparent rotational correlation time (Φ_A = 5.66 ns) obtained from the Perrin plot (Fig. 5) is the result of the global motion of the protein matrix and of that of the Trp residues. Our results indicate that orosomucoid presents two different dynamic domains, one rigid near the binding site of TNS and the second mobile near the Trp residues. We are not able from the present work to identify the position of the TNS on the protein. Some interaction may exist between the extrinsic probe and the carbohydrate residues, which can inhibit any residual motion of the probe.

It was found that binding of propranolol to orosomucoid–ANS complex induces a partial decrease in the fluorescence intensity of the probe. Substantial dye remains bound even in the presence of saturating concentrations of propranolol, suggesting that the two ligands do not have the same binding site [20]. However, ethanol caused a decrease in dye fluorescence to zero, indicating a competitive inhibition [20]. Binding of progesterone to orosomucoid inhibits Trp residues fluorescence. The extent of quenching (17%) [8] is lower than that reported for ANS (30%) [20]. This may indicate that the two ligands do not bind on the same site or it may just indicate that energy transfer between Trp and ANS is more important than energy transfer between Trp and progesterone. Fluorescence of TNS and ANS is sensitive to modifications occurring in the microenvironment of the probe. Thus it is possible to use TNS instead of ANS to reveal any structural or conformational change occurring in orosomucoid.

It is known that in general, dynamics of proteins are important to their functions [21,22]. Our next goal is to study the interaction of orosomucoid with its ligands, progesterone, propranolol and ethanol. Red-edge excitation spectra and polarization measurements on Trp residues and TNS will allow us to see whether the binding of the ligands affects the motion of the protein. In this way it will be possible to put into evidence the relation that could exist between function and dynamics of orosomucoid.

Acknowledgements

The author wishes to thank Dr. H. Debray for the preparation of orosomucoid, Professor Y. Engelborghs and Dr. K. Wilaert for the measurement of fluorescence lifetimes and the referee for his positive comments and constructive criticism. The technical assistance of the following undergraduate students is also acknowledged: S. Lemaire, C. Asseman, J. Broutin, N. Vramboudt, D. Dobel and L. Lesquin.

References

1 J.R. Lakowicz, G. Laczko, I. Gryczynski and H. Cherek, J. Biol. Chem. 261 (1986) 2240–2245.
2 J.R. Lakowicz and S. Keating-Nakamoto, Biochemistry 23 (1984) 3013–3021.
3 E. Bucci, C. Fronticelli, K. Flanigan, J. Perlman and R.F. Steiner, Biopolymers 18 (1979) 1261–1276.
4 J.R. Lakowicz and G. Weber, Biochemistry 12 (1973) 4171–4179.
5 J.R. Lakowicz and H. Cherek, Biochem. Biophys. Res. Commun. 99 (1981) 1173–1178.
6 Ch. Mohan-Rao, S. Chenchal Rao and P. Bheema Rao, Photochem. Photobiol. 50 (1989) 399–402.
7 A.P. Demchenko, FEBS lett. 182 (1985) 99–102.
8 T. Kute and U. Westphal, Biochim. Biophys. Acta 420 (1976) 195–213.
9 M. Ganguly, R.H. Carnigham and U. Westphal, Biochemistry. 6 (1967) 2803–2814.
10 W.O. McClure and G.M. Edelman, Biochemistry 5 (1965) 1908–1918.
11 J.R. Lakowicz, Principles of fluorescence spectroscopy (Plenum, New York, NY, 1983) p. 44.
12 C.B. Peterson and M.N. Blackburn, J. Biol. Chem. 260 (1985) 610–615.
13 R.D. Spencer, Ph.D. Thesis: Fluorescence lifetimes: theory, instrumentation and application of nanosecond fluorometry, Univ. of Illinois at Urbana-Champaign, (University Microfilms Int., Ann Arbor, MI, 1970).

14 E. Gratton, M. Linkeman, J.R. Lakowicz, B.P. Maliwal, H. Cherek and G. Laczko, Biophys. J. 46 (1984) 479–486.
15 D.M. Jameson, E. Gratton and R.D. Hall, Appl. Spectrosc. Rev., 20 (1984) 55–106.
16 K. Clays, J. Jannes, Y. Engelborghs and A. Persoons, J. Phys. E. Sci. Instrum. 22 (1989) 297–305.
17 P.M. Mulqueen and M.J. Kronman, Arch. Biochem. Biophys. 215 (1982) 28–39.
18 S.J. Perkins, J.-P. Kerckaert and M.H. Loucheux-Lefebvre, Eur. J. Biochem. 147 (1985) 525–531.
19 G. Weber, Biochem. J. 51 (1952) 145–155.
20 T.F. Busby and I.C. Kenneth, Biochim. Biophys. Acta 871 (1986) 61–71.
21 H. Frauenfelder, C.A. Petsko and D. Tsernoglou, Nature 280 (1979) 558–563.
22 M. Karplus and J.A. McCammon, Annu. Rev. Biochem. 53 (1983) 263–300.